IL NUOVO CIMENTO Vol. 34 C, N. 2 Marzo-Aprile 2011
DOI 10.1393/ncc/i2011-10834-9

Colloquia: WISH2010

Particle production in pp collisions at the LHC as studied by CMS

N. van Remortel on behalf of the CMS Collaboration
University of Antwerpen - Antwerpen, Belgium

(ricevuto il 17 Novembre 2010; approvato il 10 Dicembre 2010; pubblicato online il 22 Marzo 2011)

Summary. — This is a report on the study of hadron production in non-single-diffractive events by using minimum bias and jet triggered data collected with the CMS experiment in the first year of LHC running. The importance of these measurements lies in the understanding of the dynamics of multi-hadron production which is described by non-perturbative QCD. The modeling via Monte Carlo generators, and their respective re-tuning, is necessary to describe the underlying event and pile-up, having impact on many measurements that rely on an accurate measurement of hadron jets or missing transverse energy. I present an overview of the inclusive single particle spectra, the yields of strange hadrons and the charged hadron multiplicity distributions measured at several center-of-mass energies that show a fast growth of particle densities at the highest energies, especially for low transverse momenta, and a strong violation of KNO scaling in large pseudorapidity intervals.

PACS 12.38.-t – Quantum chromodynamics.
PACS 12.38.Aw – General properties of QCD (dynamics, confinement, etc.).
PACS 12.38.Qk – Experimental tests.

1. – General considerations

Each time a new collider is commissioned a re-measurement of processes with the highest cross-sections takes place. This is not only necessary in order to test and calibrate the experimental apparatus and reconstruction algorithms that grow each generation in complexity, but also to test the extrapolations of these cross-sections and the corresponding theoretical predictions into an uncharted energy domain. Generally a high-energy hadron-hadron interaction, as is the case at the LHC, occurs as seen in the rest frame of the target via the development of a cascade where the virtuality of the system degrades by the emission of partons that can be initially described with perturbative QCD (pQCD). In rare cases, a collision occurs where the virtuality has remained large, which then results in the production of objects (known or unknown) with large transverse masses, resulting in final states with high transverse momentum that can be relatively accurately calculated.

However, in a large majority of the cases the cascade enters a regime where the strong coupling is large and in which the radiation cloud has acquired transverse dimensions comparable to the target, and the perturbative description breaks down. Due to the

compositness of hadrons, soft partonic interactions also occur between the remainders of the protons when a hard partonic scatter occurs. Together with the soft initial and final state radiation of partons, the produced hadrons from the additional soft processes populate the so-called "underlying event" (UE). Another complication arises at high energies whenever the momentum transfer in a $2 \to 2$ parton scattering becomes as small as a few GeV. At this point the perturbative parton-parton scattering cross-section exceeds the total proton-proton cross-section. This introduces the concept of multiple parton interactions [1, 2] where one assumes that two or more independent semi-hard parton-parton scatters simultaneously occur in one proton-proton interaction.

Before the first LHC measurements uncertainties on the total cross-sections, inclusive single particle densities, average transverse momentum and average charged multiplicity ranged between 20–50% at an energy scale of 10 TeV [3, 4]. Most of these discrepancies are due to the lack of understanding of soft hadronic processes and in particular soft multi-hadron production.

The inter-relationship between seemingly unrelated measurements such as total cross-sections, single particle spectra and multiplicities is discussed in depth in [5]. Current models of high-energy hadron-hadron interactions apply a combination of perturbative QCD calculations to describe the hard scattering component of the interaction with phenomenological models describing the soft component relying on general principles such as duality, unitarity, Regge behavior and the parton structure of hadrons. As the LHC kinematics allow us to probe further the smaller momentum fraction soft partons in the proton, an additional need arises to take into account nonlinear effects in the parton densities and their evolution. It is an enormously challenging task for Monte Carlo generators to accommodate all these complications, though a few succeed remarkably well, in particular PYTHIA [6] and PHOJET [7, 8].

2. – Triggers and selections

A first series of CMS results on single particle spectra was published short after the first data taking of stable proton-proton collisions at $\sqrt{s} = 0.9$ and 2.36 TeV in the end of 2009 [9] and at $\sqrt{s} = 7$ TeV in the beginning of 2010 [10]. A detailed description of the CMS detector, algorithms and performances can be found in [11]. Two main subsystems were involved in the trigger of the detector readout: the Beam Scintillator Counters (BSC), two sets of 16 scintillator tiles on each side of the interaction point at a distance of 10.86 m; and the Beam Pick-up Timing for eXperiments (BPTX), located around the beam pipe at a distance of 175 m from the interaction point and designed to provide precise information on the structure and timing of the LHC beams. Minimum bias data are selected by requiring a signal in both BSC counters, in coincidence with BPTX signals from both beams. Finally, events are required to have at least one well-reconstructed primary vertex. The details of the vertex quality selection can be found in [9]. The contamination due to non-collision events that consist of beam gas interactions, beam halo and cosmic muons were estimated by analyzing events with an unpaired single bunch crossing the interaction point. The contamination was found to be below 0.1%. All data were collected during runs with low instantaneous luminosities where the interaction rate remained below 50 Hz. At these rates the probability for pile-up collisions is less than 0.3%. At $\sqrt{s} = 7$ TeV a total integrated luminosity of 1.1 μb^{-1} was analyzed.

In order to increase the statistical sensitivity for charged tracks at the highest transverse momenta, up to $p_T = 140$ GeV, two additional jet triggered data samples were analyzed with transverse energy thresholds of 15 GeV and 50 GeV. Jets are reconstructed

from calorimeter deposits using the anti-k_T algorithm [12] with $R = 0.5$. At $\sqrt{s} = 7\,\text{TeV}$ an integrated luminosity of $10.2\,\text{nb}^{-1}$ was analyzed for this purpose.

3. – Charged particle tracking

All analyses described here rely exclusively on the tracking of charged particles using the CMS silicon tracking detector, consisting of 1440 pixel detector modules and 15148 silicon strip detector modules arranged in 13 concentric layers around the interaction point in the barrel region and 14 endcap disks. The geometrical acceptance of the tracker extends to a pseudorapidity of $|\eta| < 2.5$ with a reconstruction efficiency of 96% for central tracks with $p_T > 0.25\,\text{GeV}/c$. In order to increase the efficiency for very low momentum tracks, two alternative track counting methods have been used. The first uses track segments reconstructed by the pixel detector. It combines a pair of hits in two out of three pixel detector layers with the primary vertex position. The differences in the angular positions of the two clusters with respect to the primary vertex are exploited to reduce the combinatorial background in a data driven way. This method extends the reconstruction of tracks with transverse momenta as low as $50\,\text{MeV}/c$. The second alternative is only used to count the number of tracks and is based on the counting of track clusters in the innermost layers of the pixel detector. Backgrounds are reduced by exploiting the relationship between the cluster size and the incident angle of the track. All measurements are corrected to the charged hadron level for inefficiencies due to the trigger and event selection procedure and for the tracking or clustering inefficiencies as a function of pseudorapidity and transverse momentum of the track. The measurements of the multiplicity distributions rely in addition on a Bayesian unfolding method, described in [13].

4. – Results

The charged particle pseudorapidity density is shown in fig. 1 for three center-of-mass energies of $\sqrt{s} = 0.9$ 2.36 and 7 TeV [9,10], together with the transverse momentum spectrum of charged particles in equally sized pseudorapidity bins that extend from central rapidity towards the forward region. The single particle densities are at lower energies in remarkable agreement with other experiments such as UA5 [14] and ALICE [15]. The transverse momentum spectra are identical in the measured pseudorapidity intervals and are well described by a Tsallis [16] function which can be used to extract the charged particle yields down to zero transverse momentum. The energy dependence of the charged particle density at zero rapidity and of the mean transverse momentum are presented in fig. 2 together with measurements at lower energies, showing a steep increase of the densities at $\sqrt{s} = 7\,\text{TeV}$. The measurement of the transverse momentum spectrum was extended to the highest possible values of $p_T \approx 140\,\text{GeV}/c$ by using jet triggers [26]. The Lorentz invariant differential cross-section of the scaled momentum, $x_T = 2p_T/\sqrt{s}$, is shown in fig. 3.

For strange particles such as K^0_S, Λ and Ξ^-, shown on the right hand side of fig. 3, the mean p_T increases with increasing particle mass and with increasing center-of-mass energy [32]. The results are also compared to previous experiments at lower energies [27-31]. The yield of strange particles is in general underestimated by Monte Carlo models such as PYTHIA, especially for the heavy strange baryons, as can be seen in fig. 4. An interesting extension of this analysis would be to measure the energy and/or multiplicity dependence of the strange/non-strange particle ratios.

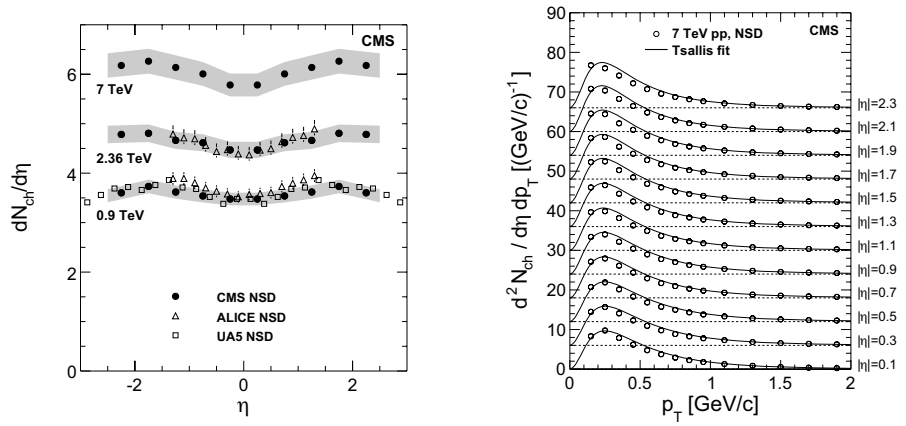

Fig. 1. – (Left) Distributions of $\mathrm{d}N_{\mathrm{ch}}/\mathrm{d}\eta$, averaged over the three measurement methods and compared with data from UA5 [14] and ALICE [15]. The shaded band shows systematic uncertainties of the CMS data. The CMS and UA5 data are averaged over negative and positive values of $|\eta|$. (Right) Differential yield of charged hadrons in the range $|\eta| < 2.4$ in 0.2-unit-wide bins of $|\eta|$ in NSD events. The solid curves represent fits to the data with the so-called Tsallis [16] function. The measurements with increasing η are successively shifted by six units along the vertical axis.

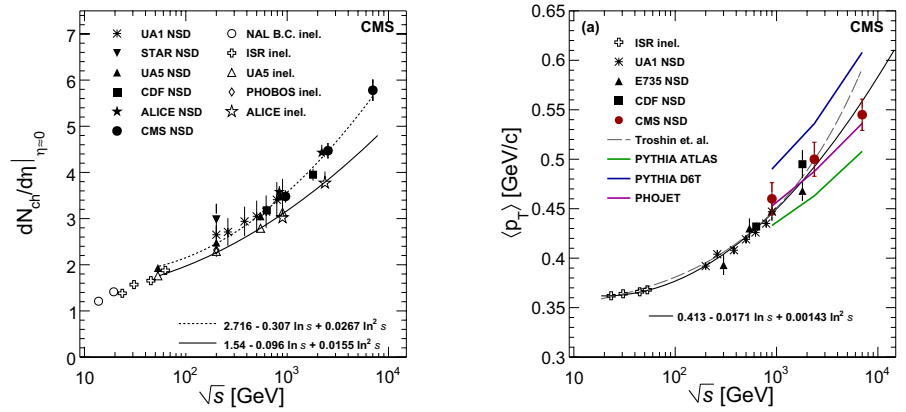

Fig. 2. – (Left) Average value of $\mathrm{d}N_{\mathrm{ch}}/\mathrm{d}\eta$ in the central η region as a function of centre-of-mass energy in pp and $\mathrm{p\bar{p}}$ collisions. Also shown are NSD and inelastic measurements from the NAL Bubble Chamber [17], ISR [18], UA1 [19], UA5 [14], CDF [20], STAR [21], PHOBOS [22], and ALICE [15]. (Right) Average p_T of charged hadrons as a function of the centre-of-mass energy. The CMS measurements are for $|\eta| < 2.4$. Also shown are measurements from the ISR [23], E735 [24], and CDF [25] for $|\eta| < 0.5$, and from UA1 [19] for $|\eta| < 2.5$. The error bars in both figures include systematic uncertainties, when available. Data points at 0.9 and 2.36 TeV are slightly displaced horizontally for visibility.

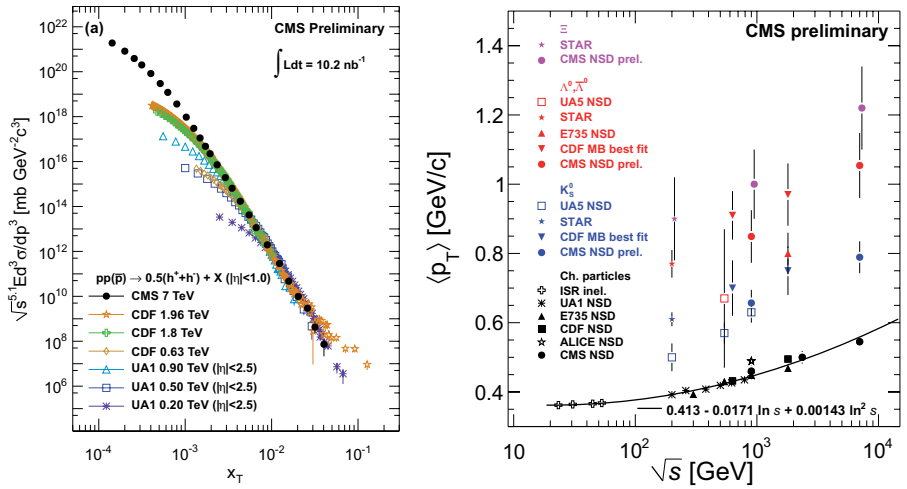

Fig. 3. – (Left) Inclusive invariant cross-sections, scaled by $\sqrt{s}^{5.1}$, for $|\eta| < 1.0$ as a function of x_T. (Right) Average p_T for charged hadrons, K^0_S, Λ^0 and Ξ^-, as a function of the center-of-mass energy. The CMS measurements are for $|y| < 2$. Also shown are the most recent results from UA5 [27, 28], E735 [29], CDF [30] and STAR [31].

The dynamics of particle production is revealed more explicitly in the charged hadron multiplicity distributions [33], P_n, as shown in fig. 5 at three center-of-mass energies and with or without a transverse momentum cut of $p_T > 500\,\text{MeV}/c$. The CMS measurements are compared with three classes of models dealing with soft multi-hadron production: PYTHIA 6 [6], PYTHIA 8 [34] and PHOJET [7, 8]. PYTHIA D6T underestimates drastically the multiplicity at all measured energies but improves when a transverse momentum cut of $p_T > 500\,\text{MeV}/c$ is applied. PYTHIA 8 is the only model that gives a reasonable description of the multiplicity distribution at all energies, but tends to over-

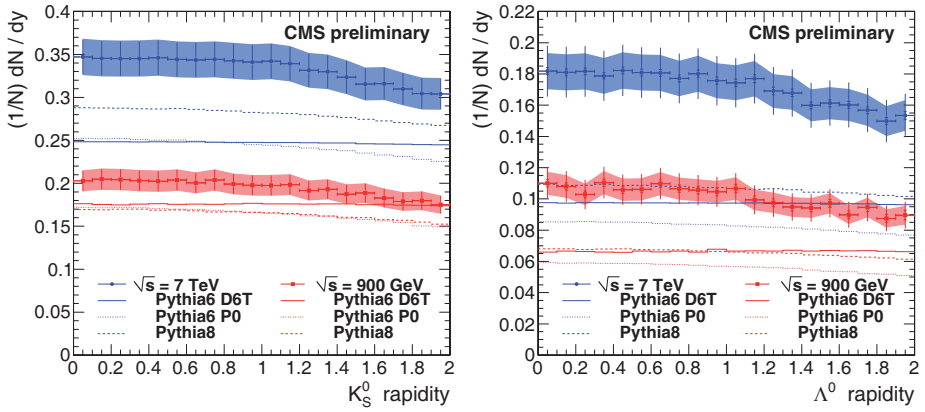

Fig. 4. – Hadron-level yield of strange particles per NSD event as a function of rapidity for the CMS data and three PYTHIA Monte Carlo samples. Neutral kaons are shown on the left, and lambdas on the right.

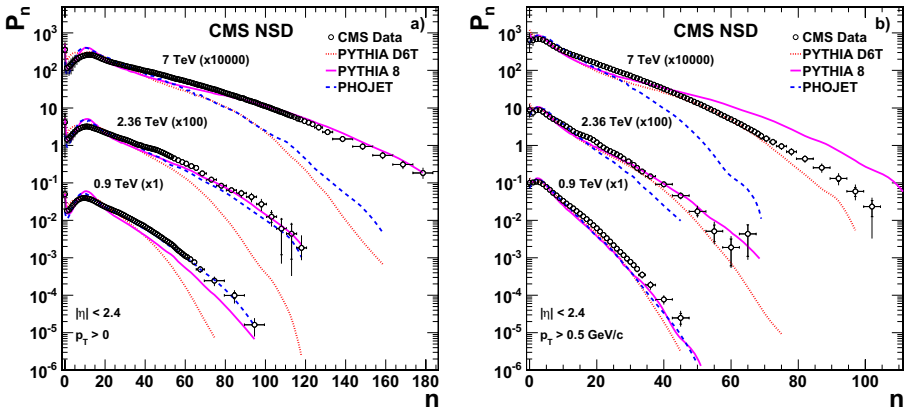

Fig. 5. – The charged hadron multiplicity distributions in $|\eta| < 2.4$ for (a) $p_T > 0$ and (b) $p_T > 500\,\mathrm{MeV}/c$, compared to two different PYTHIA models and the PHOJET model at $\sqrt{s} = 0.9$, 2.36, and 7 TeV. Results for different center-of-mass energies are scaled with a multiplicative factor for clarity.

estimate the multiplicity at 7 TeV when $p_T > 500\,\mathrm{MeV}/c$ is required. PHOJET produces too few charged hadrons overall but gives a good description of the average transverse momentum $\langle p_T \rangle$ at fixed multiplicity n, as illustrated in fig. 6. Among the three classes of models, PYTHIA 8 gives the best overall description of the multiplicity distribution and the dependence of the average transverse momentum on n. Traditionally, the s dependence of P_n and its moments has been much discussed [38, 5, 4] in relation to Koba-Nielsen-Olesen (KNO) scaling [39, 40]. In this framework one studies the KNO function $\Psi(z) = \langle n \rangle P_n$, where $z = n/\langle n \rangle$. If KNO scaling holds, $\Psi(z)$ and the normalized moments $C_q = \langle n^q \rangle / \langle n \rangle^q$ are independent of s. At the highest energies, KNO scaling is observed to hold quite well for small pseudorapidity intervals of $|\eta| < 0.5$ but

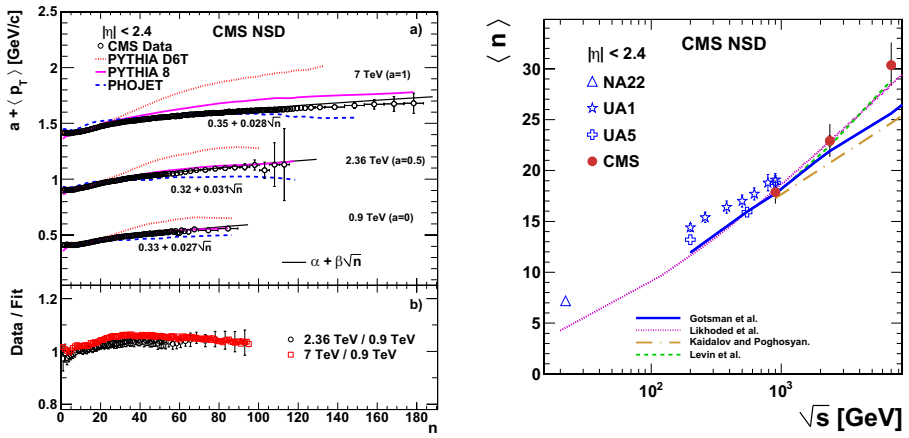

Fig. 6. – A comparison of $\langle p_T \rangle$ *vs.* n for $|\eta| < 2.4$ with two different PYTHIA models and the PHOJET model at $\sqrt{s} = 0.9$, 2.36, and 7 TeV (left). Results for different energies are shifted for reasons of clarity. The evolution of the mean charge multiplicity with the center-of-mass energy for $|\eta| < 2.4$, including data from lower energy experiments for $|\eta| < 2.5$ [35-37, 19] (right).

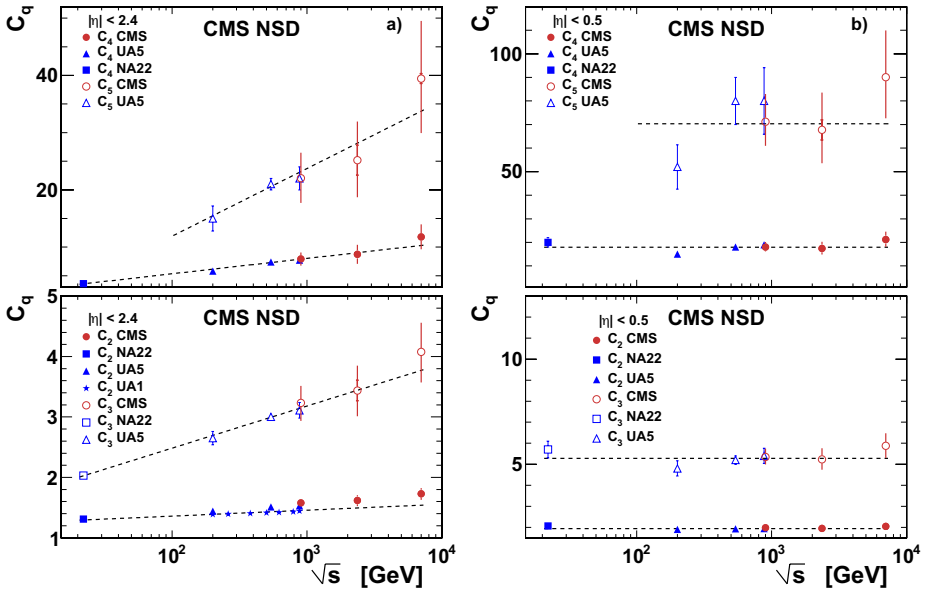

Fig. 7. – Fits of the $\ln s$ dependence of the normalized moments C_q of the multiplicity distribution for (a) $|\eta| < 2.4$ (assuming linear dependence) and (b) $|\eta| < 0.5$ (assuming constant dependence), including data from lower energy experiments [35-37].

is strongly violated for larger pseudorapidity domains. This is quantified explicitly by the energy dependence of the C_q moments shown in fig. 7, which shows a linear growth in $\ln s$ for a pseudorapidity interval $|\eta| < 2.4$ and no energy dependence for $|\eta| < 0.5$.

5. – Conclusions

A detailed analysis of minimum bias data is essential in order to achieve a correct modeling of the largest part of the proton-proton interaction cross-section. Soft QCD events will constitute the pile-up events at high instantaneous luminosities at the LHC and their physics is similar to the underlying event that will complicate accurate measurements of jet energies and missing transverse energy. In addition we can learn new things about the non-perturbative regime of QCD. Some small surprises in the first CMS data include a strong rise of the charged particle densities at the highest center-of-mass energy, the observation of an increased amount of heavy strange hadrons, the indication of a multi-component structure in the multiplicity distributions and a strong violation of KNO scaling in large pseudorapidity intervals.

REFERENCES

[1] Sjostrand T. and van Zijl M., *Phys. Lett. B*, **188** (1987) 149.
[2] Sjostrand T. and van Zijl M., *Phys. Rev. D*, **36** (1987) 2019.
[3] Moraes A., Buttar C. and Dawson I., *Eur. Phys. J. C*, **50** (2007) 435.
[4] Grosse-Oetringhaus J. and Reygers K., *Charged-Particle Multiplicity in Proton-Proton Collisions*, arXiv:0912.0023 (2009).

[5] Kittel W. and De Wolf E. A., *Soft Multihadron Dynamics* (World Scientific, Hackensack, USA) 2005.
[6] Sjostrand T., Mrenna S. and Skands P. Z., *JHEP*, **05** (2006) 026.
[7] Engel R., *Z. Phys. C*, **66** (1995) 203.
[8] Engel R. and Ranft J., *Phys. Rev. D*, **54** (1996) 4244.
[9] Khachatryan V. *et al.*, *JHEP*, **02** (2010) 041.
[10] Khachatryan V. *et al.*, *Phys. Rev. Lett.*, **105** (2010) 022002.
[11] Adolphi R. *et al.*, *JINST*, **3** (2008) S08004.
[12] Cacciari M., Salam G. P. and Soyez G., *JHEP*, **04** (2008) 063.
[13] D'Agostini G., *Nucl. Instrum. Methods A*, **362** (1995) 487.
[14] Alner G. J. *et al.*, *Z. Phys. C*, **33** (1986) 1.
[15] Aamodt K. *et al.*, *Eur. Phys. J. C*, **68** (2010) 89.
[16] Tsallis C., *J. Stat. Phys.*, **52** (1988) 479.
[17] Whitmore J., *Phys. Rep.*, **10** (1974) 273.
[18] Thome W. *et al.*, *Nucl. Phys. B*, **129** (1977) 365.
[19] Albajar C. *et al.*, *Nucl. Phys. B*, **335** (1990) 261.
[20] Abe F. *et al.*, *Phys. Rev. D*, **41** (1990) 2330.
[21] Adams J. *et al.*, *Phys. Rev. C*, **73** (2006) 034906.
[22] Nouicer R. *et al.*, *J. Phys. G*, **30** (2004) S1133.
[23] Rossi A. M. *et al.*, *Nucl. Phys. B*, **84** (1975) 269.
[24] Alexopoulos T. *et al.*, *Phys. Rev. Lett.*, **60** (1988) 1622.
[25] Abe F. *et al.*, *Phys. Rev. Lett.*, **61** (1988) 1819.
[26] CMS Collaboration, CMS NOTE PAS QCD-10-008 (2010).
[27] Ansorge R. E. *et al.*, *Phys. Lett. B*, **199** (1987) 311.
[28] Alner G. J. *et al.*, *Nucl. Phys. B*, **258** (1985) 505.
[29] Banerjee S. *et al.*, *Phys. Rev. Lett.*, **62** (1989) 12.
[30] Acosta D. *et al.*, *Phys. Rev. D*, **72** (2005) 052001.
[31] Abelev B. I. *et al.*, *Phys. Rev. C*, **75** (2007) 064901.
[32] CMS Collaboration, CMS NOTE PAS QCD-10-007 (2010).
[33] CMS Collaboration, CMS NOTE PAS QCD-10-004 (2010).
[34] Sjostrand T., Mrenna S. and Skands P. Z., *Comput. Phys. Commun.*, **178** (2008) 852.
[35] Adamus M. *et al.*, *Z. Phys. C*, **37** (1988) 215.
[36] Alner G. J. *et al.*, *Phys. Lett. B*, **160** (1985) 193.
[37] Ansorge R. E. *et al.*, *Z. Phys. C*, **43** (1989) 357.
[38] De Wolf E. A., Dremin I. M. and Kittel W., *Phys. Rep.*, **270** (1996) 1.
[39] Koba Z., Nielsen H. B. and Olesen P., *Nucl. Phys. B*, **40** (1972) 317.
[40] Hegyi S., *Nucl. Phys. Proc. Suppl.*, **92** (2001) 122.